Available online at www.sciencedirect.com
SCIENCE DIRECT®
Journal of Power Sources 129 (2004) 143–151
JOURNAL OF POWER SOURCES
www.elsevier.com/locate/jpowsour

Control of miniature proton exchange membrane fuel cells based on fuzzy logic

J.O. Schumacher [a,*], P. Gemmar [b], M. Denne [b,1], M. Zedda [a], M. Stueber [b]

[a] *Department of Energy Systems, Fraunhofer Institute for Solar Energy Systems ISE, Heidenhofstrasse 2, 79110 Freiburg, Germany*
[b] *Institute for Innovative Computer Science Applications (i3A), University of Applied, Sciences FH Trier, Schneidershof, 54293 Trier, Germany*

Received 21 May 2003; received in revised form 13 October 2003; accepted 20 October 2003

Abstract

A control strategy is presented in this paper which is suitable for miniature hydrogen/air proton-exchange membrane (PEM) fuel cells. The control approach is based on process modelling using fuzzy logic and tested using a PEM stack consisting of 15 cells with parallel channels on the cathode side and a meander-shaped flow-field on the anode side. The active area per cell is 8 cm^2. Commercially available materials are used for the bipolar plates, gas diffusion layers and the membrane-electrode assembly (MEA). It is concluded from a simple water balance model that water management at different temperatures can be achieved by controlling the air stoichiometry. This is achieved by varying the fan voltage for the air supply of the PEM stack. A control strategy of the Takagi Sugeno Kang (TSK) type, based on fuzzy logic, is presented. The TSK-type controller offers the advantage that the system output can be computed in an efficient way: the rule consequents of the controller combine the system variables in linear equations. It is shown experimentally that drying out of the membrane at high temperatures can be monitored by measuring the ac impedance of the fuel cell stack at a frequency of 1 kHz. Flooding of single cells leads to an abrupt drop of the corresponding single-cell voltage. Therefore, the fuzzy rule base consists of the ac impedance at 1 kHz and all single-cell voltages. The parameters of the fuzzy rule base are determined by plotting characteristic diagrams of the fuel cell stack at constant temperatures. The fuel cell stack can be controlled at $T = 60\,^{\circ}C$ up to a power level of 7.5 W. The fuel cell stack is controlled successfully even when the external electric load changes. At $T = 65\,^{\circ}C$, a maximum power level of 8 W is found. A decrease of the maximum power level is observed for higher temperatures.

Keywords: Proton exchange membrane fuel cell; PEM fuel cell; System control; Fuzzy logic; Portable power supply

1. Introduction

Miniature fuel cells are being developed at Fraunhofer ISE as alternatives to rechargeable batteries, like e.g. lithium-ion batteries, in portable electronic devices. In order to ensure a reliable power source, a control scheme for the fuel cell stack is needed. Especially, water and thermal management of miniature proton-exchange membrane (PEM) fuel cells are critical issues, which have to be addressed by the control strategy.

An efficient control strategy for miniature PEM fuel cells should be based on a minimum number of peripheral components. Humidifiers and water cooling devices cannot be considered for a cost-effective, low-weight portable fuel cell system. The diagnostics of the fuel cell stack should be based on electrical measurements. These can be made more accurately and are less prone to failure than sensors (e.g. humidity sensors). The air supply for our miniature PEM fuel cells is achieved by fans rather than pumps. Fans offer the advantage of a lower power consumption in comparison to pumps.

A model-based control strategy would be desirable, which takes the transient response of the fuel cell to load changes of the power consumer into account. Using such a control strategy, the effort of adapting the parameters of the model to the specific design of the fuel cell and the peripheral components of the system could be minimised. We review the state of model-based control strategies for PEM fuel cells in Section 2.

In practice, problems during the operation of a portable fuel cell system occur after a change of the power load of the electronic device. Typically, the load changes on a time

* Corresponding author.
E-mail addresses: schum@ise.fhg.de (J.O. Schumacher), gemmar@i3A.fh-trier.de (P. Gemmar), denne_matthias@t-online.de (M. Denne), stueber@i3A.fh-trier.de (M. Stueber).
URLs: http://www.ise.fhg.de, http://www.i3a.fh-trier.de.
[1] Present address: IS Software GmbH, Nordring 26, 90408 Nuernberg, Germany.

0378-7753/$ – see front matter © 2003 Elsevier B.V. All rights reserved.
doi:10.1016/j.jpowsour.2003.10.010

scale of milliseconds, followed by a peak power demand for several seconds up to minutes. After a load change, for example the rate of water production on the cathode side of the fuel cell increases. The main purpose of the control strategy is to ensure uninterrupted operation of the fuel cell stack for changing power demand.

The use of fuzzy methods for system control is discussed in Section 3. Basic thermodynamic considerations for the water management of PEM fuel cells can be found in Section 4. We proceed with an explanation of our experimental set-up in Section 5. The stack design is also discussed here. Characteristic diagrams of this fuel cell stack were plotted at different temperatures (Section 6). Our fuzzy-based control approach is presented in Section 7 including a detailed explanation of the fuzzy rule base for the water management. The control approach is tested for changing load conditions over a time range of minutes.

2. Model-based control strategies

The transient response of a PEM fuel cell to a load change of the power consumer is a complex phenomenon. A transient model has to account for the electrochemical reaction of the fuel and air and multi-phase transport of water and the gas components. Moreover, heat and charge transport occur in PEM fuel cells.

Steady-state mathematical models of PEM fuel cells have been presented by several authors [1–3]. Steady-state models are not applicable for model-based control strategies because load changes of the power-consuming device cannot be taken into account. Moreover, most of the recent models are computationally expensive and therefore difficult to apply to the control of fuel cells [4,5]. On the other hand, most control-oriented models are based on simplified versions of comprehensive fuel cell models.

A one-dimensional dynamic model has been presented by Ceraolo et al. [6]. All quantities vary only in the direction orthogonal to the electrode surfaces. The model accounts for multi-component gas diffusion in the porous backing layers, cathode kinetics and double layer charging. The dynamic cell response to current steps can be reproduced by the model. However, cathode flooding cannot be described by the single-phase model. Therefore, water management cannot be achieved using this model.

A control-oriented dynamic model of a pressurised fuel cell system for application in vehicles has been presented by Pukrushpan et al. [7]. The terminal voltage of the fuel cell stack is modelled on the basis of the load current and operating conditions, including cell temperature, air pressure and oxygen partial pressure. Flow equations, mass and energy balance and electrochemical reactions were used to create a lumped dynamic model of the fuel cell cathode. The fuel cell stack characteristics are given as a function of activation losses, ohmic losses and concentration losses. The coefficients in the overvoltage expressions are functions of temperature, pressure and oxygen partial pressures. However, the authors assume a 100% humidified membrane in order to reduce the model‘s complexity. This assumption is over-simplified as our measurement results show. Drying of the membrane may well occur in our fuel cell system for high fan voltages, as shown in Section 6.2.

Another dynamic fuel cell system model for automotive vehicle simulation and control is described by Boettner et al. [8]. Voltage-current density relationships were analysed using the system analysis program Gctool [9]. The effects of cathode pressure and fuel cell operating temperature on fuel cell voltage, power density, and exergetic efficiency were analysed. Moreover, models of auxiliary components required for fuel cell stack functionality were developed and integrated into a vehicle performance simulator. Driving cycles and the start-up behaviour of the fuel cell system was investigated. The focus of the paper is on the optimisation of the exergetic efficiency, water management is not addressed there.

Abtahi et al. presented a control strategy of a fuel cell system based on a pressure regulator [10]. Different pulsing profiles for the pulsed air source were investigated. The pulse amplitude, the frequency and the duty cycles were varied and the impact on the fuel cell power density was studied. The authors discuss the applicability of fuzzy logic in order to implement a control strategy. Pulsing of the air pressure cannot be applied in our fuel cell system because we use fans for the air supply.

3. Fuzzy control principle

All processes of nature or technology contain more or less uncertain components or have an uncertain outcome. For example, many technical processes cannot be characterised accurately by analytical approaches or can only be described using vague terms. With the formulation of Fuzzy Theory by Zadeh, a mathematical method for the formulation of uncertainty was introduced [11].

Over the past few decades fuzzy methods have proven to be successful in many industrial and non-industrial applications. Especially in the field of modelling and controlling dynamic processes, where traditional methods had been preferred, fuzzy methods are now favoured. With the advent of new technologies, practical requirements where classical methods fail arise increasingly often, either because exact models are not present or because a closed mathematical description is not available or too expensive.

By contrast, fuzzy methods make it possible to exploit available expert knowledge or to extract process information from measured data and then to describe the behavior of even complex processes in a linguistic form. The expert's assessments or process description can be abstracted from technical descriptions in the form of *IF* ... *THEN* ... rules like *IF temperature = high AND voltage = very_low THEN air_pressure = high* [12]. Fuzzy logic enables the

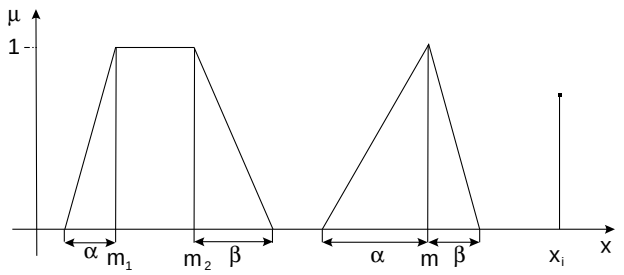

Fig. 1. Trapezoidal, triangular and singleton membership functions μ_X (α, β, m, m_1, m_2: description parameters).

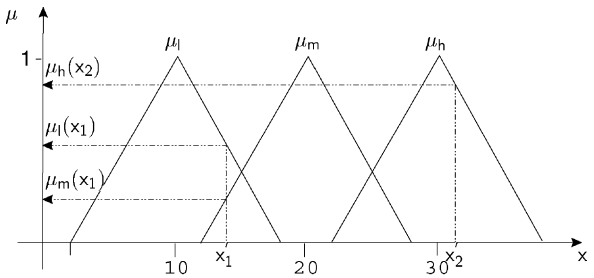

Fig. 2. Example: Linguistic variable x with linguistic terms (fuzzy sets) low (μ_l), medium (μ_m), high (μ_h), and fuzzification of x'_1, x'_2.

description of process models and control in a way very similar to human thinking.

3.1. Fuzzy set and membership function

In classical (Cantor) set theory, an element x belongs to a subset X ($x \in X$) or it does not ($x \notin X$), which can be expressed by a binary characteristic function $\chi_X : B_x \rightarrow \{0, 1\}$, where B_x is the base set of X. By contrast, fuzzy logic assigns a *degree* $\mu_X(x)$ in the interval $[0, 1]$ for every element $x \in X$ thus specifying how well x matches the characteristic of X. $\mu_X(x)$ is called a membership function $\mu_X : B_x \rightarrow [0, 1]$ and describes a fuzzy (sub-) set X for a fuzzy variable x. Fuzzy sets can be specified in various ways: graphically, analytically or numerically by discrete pairs (singletons) $\mu_X(x_i)/x_i$. In practice, simple geometric functions are mainly used (Fig. 1).

3.2. Fuzzy inference

A fundamental application of fuzzy logic is *Fuzzy Inference* or *Approximate Reasoning*. It describes fuzzy logical reasoning based on uncertain information, in the form of *IF* < *premise* > *THEN* < *consequent* > rules. The premise part describes the rule antecedent as a fuzzy logical expression with fuzzy input variables x_i (*linguistic variables*), which have been partitioned by one or more fuzzy sets X_i (*linguistic terms*; here we consider one appropriate fuzzy set X_i per variable x_i and rule R) and their corresponding membership functions μ_i, respectively. If the premise uses $n > 1$ input variables of not necessarily the same base sets B_{x_i}, they are normally combined by an n-ary fuzzy *AND* operator. The consequent part of rule R describes a fuzzy set Y of output variable y over base set B_y:

$$R : IF\ \ x_1 = X_1\, AND \ldots AND\, x_n = X_n\, THEN\ \ y = Y \quad (1)$$

If the fuzzy *AND* operator is modelled with the minimum function *MIN* (*t-norm*), then the resulting fuzzy set Y' is obtained as a clipped fuzzy set Y. Clipping $Y \mapsto Y' \in [0 \ldots H]$ is achieved by thresholding fuzzy set Y at level H specified by the output of the *MIN* function. Thus, rule R can be interpreted as an n-ary relation R over the fuzzy inference pattern:

$$\begin{aligned} R : \mu_{Y'}(y) &= \mu_R(x'_1, x'_2, \ldots, x'_n, y) \\ &= MIN(\mu_1(x'_1), \mu_2(x'_2), \ldots, \mu_n(x'_n), \mu_Y(y)), \\ & \qquad y \in B_y. \end{aligned} \quad (2)$$

One calls $H = MIN(\mu_1(x'_1), \ldots, \mu_n(x'_n))$ the *weight* or *degree of match* of rule R for the current event $X' = (x'_1, \ldots, x'_n)$ and $\mu_i(x'_i)$ are the *fuzzifications* of the actual and sharp inputs x'_i (Fig. 2).

Using this formal framework, Fuzzy Linguistics defines elements for the (verbal) description of fuzzy quantities used to handle vague or uncertain information. Linguistic variables identify the characteristic quantities of a system and their definition space is partitioned by linguistic terms like low, medium and high, defined by the corresponding fuzzy (sub-) sets μ_l, μ_m, μ_h, (Fig. 2). In this way, linguistic expressions like *IF* x_1 = *medium AND* x_2 = *low THEN* y = *high* describe part of a problem solution (e.g. fuzzy rule-based system, Section 3.3) and fuzzy implications provide the corresponding computational method.

3.3. Fuzzy rule-based systems

A fuzzy rule-based system consists of a system of inference rules (implications) and an inference pattern. It produces sharp or crisp outputs y from crisp inputs x'_i. The system of inference rules represents a rule base $\{R_k\}$ with m rules ($k = 1, \ldots, m$).

$$R_k : IF\ \ x_1 = X_{k1}\ \ AND \ldots AND\ \ x_n = X_{kn}\ \ THEN\ \ y = Y_k. \quad (3)$$

Evaluation of the rule base is carried out by *OR*-combination of the individual rules R_k. In practice, the maximum function *MAX* is used as an appropriate model for fuzzy *OR* functions (t-conorm):

$$R_1 \cup \ldots \cup R_m : \mu_{\mathrm{res}}(y) := MAX(\mu_{Y'_1}(y), \ldots, \mu_{Y'_m}(y)). \quad (4)$$

Thus one gets a resulting fuzzy set $\mu_{\mathrm{res}}(y)$ as the maximum function of the clipped fuzzy sets $\mu_{Y'_k}$ (Eq. (2)). Finally, a crisp value y_{res} is achieved by defuzzification of $\mu_{\mathrm{res}}(y)$

(e.g. y-coordinate of centre of gravity of $\mu_{\text{res}}(y)$). It was shown [13], that any continuous non-linear function can be approximated as exactly as needed with a finite set of fuzzy variables, sets and rules.

3.4. Fuzzy controller

Fuzzy rule bases (Eq. (3)) are used for modelling or controlling processes. With respect to the type of consequent part used, one can differentiate between two major approaches:

1. Mamdani controllers: both the premise and consequent variables are linguistic variables and characterised by corresponding linguistic terms (fuzzy sets, membership functions, (Eq. (3))) [14].
2. Takagi Sugeno Kang (TSK) controllers: Only the premise variables are linguistic variables with corresponding linguistic terms. The consequent part uses crisp (original) variables combined in a linear function (5) [15].

A fuzzy rule base $\{R_k\}$ of TSK type is established by rules of the following type:

$$R_k : IF\ \ x_1 = X_{k1}\ \ AND\ \ x_2 = X_{k2} \ldots AND\ \ x_n = X_{kn}\ \ THEN\ \ y_k = p_{k0} + p_{k1}x_1 + p_{k2}x_2 + \ldots + p_{kn}x_n. \quad (5)$$

The resulting system output of a TSK fuzzy model is calculated as the average of the crisp rule outputs y_k weighted by the degree of rule matches H_k:

$$y_{\text{res}} = \frac{\sum_{i=1}^{m} H_i y_i}{\sum_{i=1}^{m} H_i}. \quad (6)$$

This avoids the critical task of defuzzification, and instead provides an easy and transparent method for manipulating and calculating the system output. Furthermore, the adaption of a TSK fuzzy model is simplified: After setting up the linguistic terms for the rule antecedents (e.g. translation of expert knowledge), the rule base can be constructed systematically. The rule consequents combine available input variables (must not be part of the premises) in linear equations with parameters p_{kl} ($k = 1, \ldots, m$; $l = 0, \ldots, n$). These parameters p_{kl} have to be optimised according to a quality function, for example. Given measured process data, the optimisation of parameters can be carried out by numerical evaluation of a system of linear equations. In the following, only fuzzy systems of TSK type are considered for modelling and controlling a fuel cell stack.

4. Water management of PEM fuel cells

Water management is crucial for undisturbed operation of PEM fuel cells and for optimisation of the output power. Flooding of the fuel cell due to excess water production blocks the gas transport towards the catalyst particles of the electrodes. On the other hand, drying of the membrane leads to a poor protonic conductivity of the PEM membrane. Consequently, an increase of resistive losses and a decrease of output power result from a low hydration state of the membrane [2,16]. Detailed water balance models were presented by Bernardi [17], Fuller [3], Nguyen and White [18] and Okada et al. [19].

A simplified water balance calculation can be found in reference [20]. The relative humidity at the cathode outlet of a PEM fuel cell is estimated using a simple model. It is assumed that the flow rate of water through the membrane due to electro-osmotic drag equals the flow rate due to back diffusion: the net water drag coefficient can be set to zero with good accuracy for our test conditions, i.e. moderate current density values and low stoichiometric values on the anode side. This was found experimentally by variation of the membrane type, the humidification of the gases, the hydrogen stoichiometry, and the current density of a PEM fuel cell in reference [21]. All product water is assumed to evaporate. Furthermore, dry air at the cathode and the validity of the ideal gas law is assumed. This yields

$$P_{\text{w}} = \frac{0.421}{\lambda + 0.188} P_{\text{t}}, \quad (7)$$

where P_{w} is the water vapour pressure at the cathode outlet, λ the air stoichiometry and P_{t} the total air pressure. The relative humidity ϕ of the air at the cathode outlet is obtained by dividing Eq. (7) by the saturated water vapour pressure $P_{\text{w}}^{\text{sat}}(T)$

$$\phi = \frac{P_{\text{w}}}{P_{\text{w}}^{\text{sat}}(T)}. \quad (8)$$

The relative humidity ϕ is plotted as a function of temperature for an air stoichiometry of $\lambda = 2$ in Fig. 3. It can be seen that (for the chosen air stoichiometry) there is only a small temperature range around $T = 60\,^{\circ}\text{C}$ which allows water management, i.e. where the air is saturated with water vapour. The fuel cell tends to be flooded with water at lower temperatures and it tends to dry out at higher temperatures.

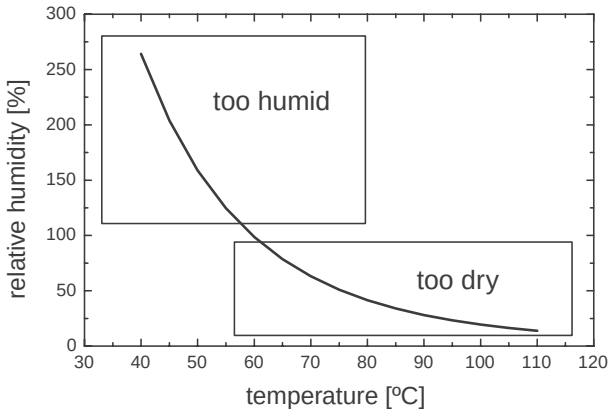

Fig. 3. Relative humidity of the air at the cathode outlet as a function of temperature ($\lambda = 2$, $P_{\text{t}} = 1$ atm).

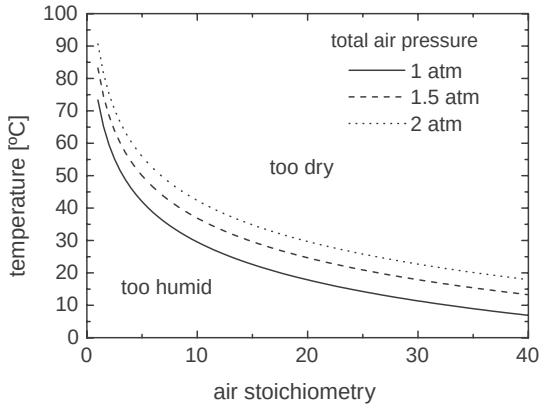

Fig. 4. Combinations of temperature vs. air stoichiometry for $\phi = 100\%$.

Solving Eq. (8) for $\phi = 100\%$ gives the lines plotted in Fig. 4. It can be concluded that water management at different temperatures can be achieved in principle by controlling the air stoichiometry. However, there is a lower temperature limit depending on the amount of air which can be supplied by the fan according to the model explained above. Moreover, there is a higher temperature limit of approximately $T = 70\,^{\circ}\mathrm{C}$ because the air stoichiometry approaches a value of 1.

5. Fuel cell stack and experimental set-up

A PEM fuel cell stack consisting of 15 cells was used in this work. The geometric dimensions of the stack are 50 mm × 25 mm × 27 mm, and the active area per cell is 8 cm^2. A flow-field with 25 mm long parallel channels on the cathode side was machined, whereas a meander-shaped flow-field on the anode side was used. All channels of the cathode flow-field are opened towards the outside. The bipolar plates were made of SGL Sigracet BMA 5. A commercially available membrane-electrode assembly (MEA) from Gore (Primea 5510) was used. Gas diffusion layers of type Toray TGP-H-060 were employed on both the anode and cathode sides. Two fans of 2 cm diameter were positioned at a distance of approximately 2 cm from the stack. The fans and the stack were mounted in a housing. A schematic diagram of the experimental set-up employed in this work is shown in Fig. 5. The electrical ac impedance Z of the stack was measured at a frequency of 1 kHz using a Hewlett Packard 4338 B. Z is mainly composed of the protonic resistance of the membrane and the internal contact resistances of the fuel cell stack [22]. Therefore, Z is a characteristic variable reflecting the humidification conditions of the fuel cell stack. The humidity of the air was measured at the cathode outlet of the stack using

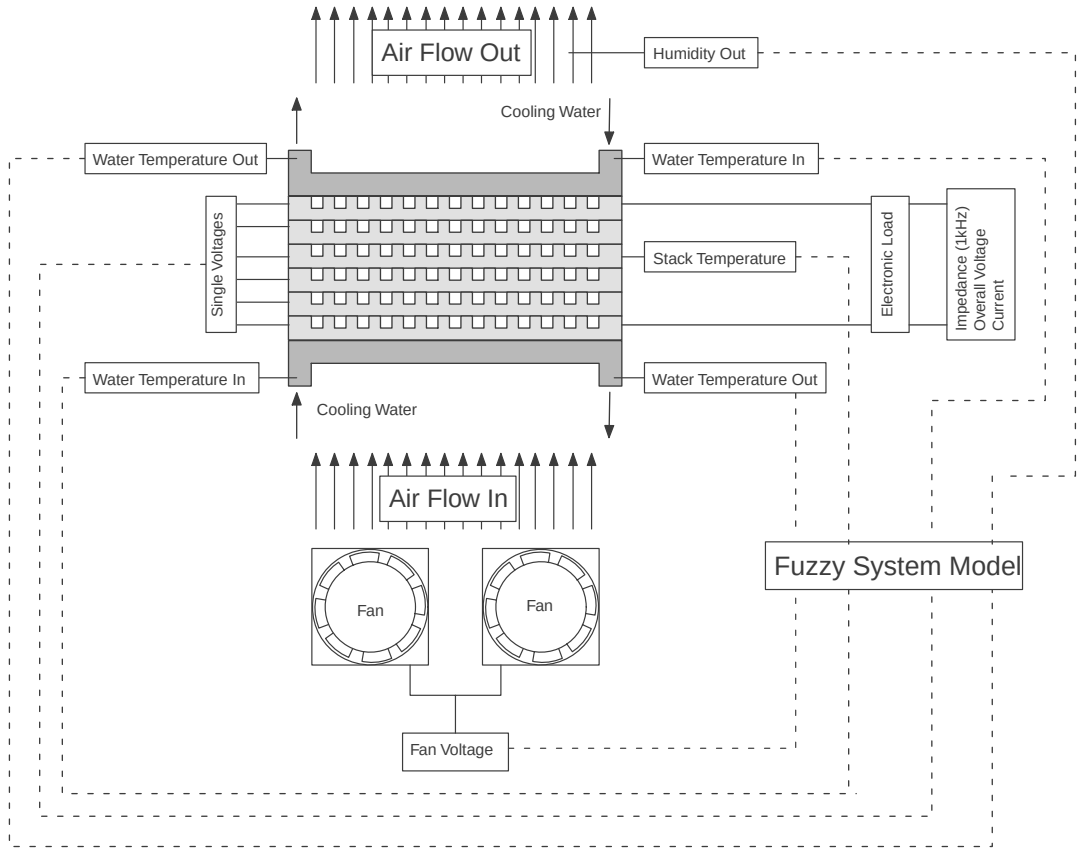

Fig. 5. The figure shows the experimental set-up including the fuel cell stack. Measurement categories and manipulated variables of the fuzzy control system are depicted as dashed lines.

a sensor of type Rotronic-Hygrometer C-94. The fuel cell stack temperature was controlled via a heating sock. The fuel cell temperature was monitored at two points, in the centre of the stack and at the cell boundary. The air stoichiometry was controlled by variation of the fan voltage. The voltage of each cell was monitored separately during the experiments.

6. Characteristic diagrams

Characteristic diagrams were plotted for constant temperature values of the stack. Data were gathered under manual control conditions. Qualitative data analysis delivered information about typical system behaviour to build up fuzzy system models, which were then optimised and tested with quantitative data.

6.1. Lower temperature limit

Fig. 6 shows part of a characteristic diagram of the fuel cell stack measured at a temperature of $T = 40\,^{\circ}\mathrm{C}$. The power load was increased at $t = 3\,\mathrm{min}$ from 3.5 to 7.5 W. This leads to a dramatic decrease in cell voltage due to water flooding problems within the cell. Additionally, it can be seen that the impedance at 1 kHz decreases due to an increase of the water content of the membrane. The problem can be partly solved by increasing the air stoichiometry ($t > 5\,\mathrm{min}$). Enough water is removed from the cell to restore the stack voltage. This leads to a power level of around 9 W (for $t \approx$ 8–12 min). The air stoichiometry was manually increased to higher values after the cell recovery. This leads to higher ohmic losses due to the increase of the stack impedance at 1 kHz. This explains the decrease of power level for $t >$ 12 min.

6.2. Higher temperature limit

Part of a characteristic diagram plotted at $T = 70\,^{\circ}\mathrm{C}$ is shown in Fig. 7. The impedance values are shifted to higher values compared to the lower temperature case because of the lower water content of the membrane. As explained in Section 4, the air stoichiometry at $T = 70\,^{\circ}\mathrm{C}$ approaches a lower limit of one in order to avoid drying of the membrane (Fig. 4). Therefore, sufficient oxygen supply can only be ensured at high temperatures with external humidification. This should be avoided in the investigated miniature fuel cell due to the expense of the additional peripheral components of a humidifier.

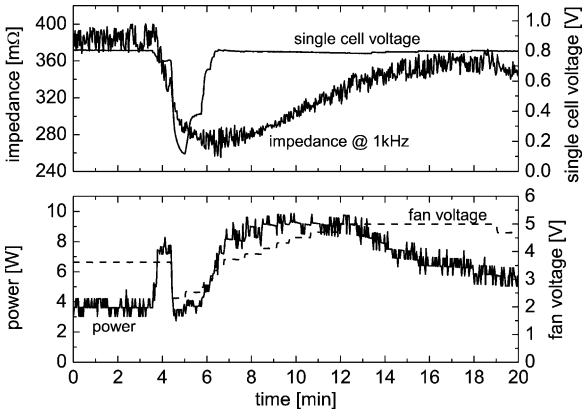

Fig. 6. Characteristic diagram at $T = 40\,^{\circ}\mathrm{C}$.

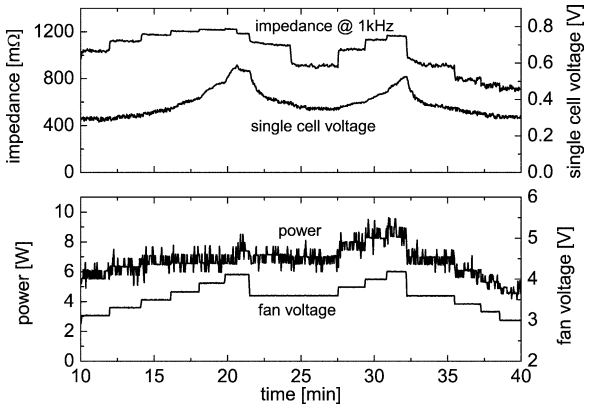

Fig. 7. Characteristic diagram at $T = 70\,^{\circ}\mathrm{C}$.

The 1 kHz impedance is highly dependent on the air stoichiometry at high temperatures as can be seen in the upper part of Fig. 7. Thus, increasing the air supply clearly leads to higher ohmic losses at this temperature. However, the power level increases due to the counteracting effect of a higher ionic current density produced by the electrochemical reaction at the cathode side. Increasing the air supply increases the oxygen concentration at the phase boundary between the electronic and the ionic conductors in the electrodes.

7. Control of the miniature PEM fuel cell stack

The control scheme is shown in Fig. 8. The fuel cell stack impedance at 1 kHz $Z_{1\,\mathrm{kHz}}$ is the controlled output variable. Furthermore, feedback from two state variables of the fuel cell stack is used by the control scheme: The minimum value $U_{\min}$ of all single-cell voltages and the derivative of the cell impedance as the difference ΔZ within the last time interval.

7.1. Fuzzy rule base for cell control of the fuel cell

Three linguistic variables, Z_{OU}, Z_{NA}, and $U_{\min}$, are used to set up the fuzzy rule base of the control scheme:

(1) It is concluded from the experimental results of Sections 6.1 and 6.2 that for stable operation, the stack impedance $Z_{1\,\mathrm{kHz}}$ should be kept within a specified range $Z_{\mathrm{spec}} = [Z_{ll} \ldots Z_{ul}]$. The impedance range which is to be chosen for optimum stack operation depends on the temperature. For example, at $T = 60\,^{\circ}\mathrm{C}$ the Z

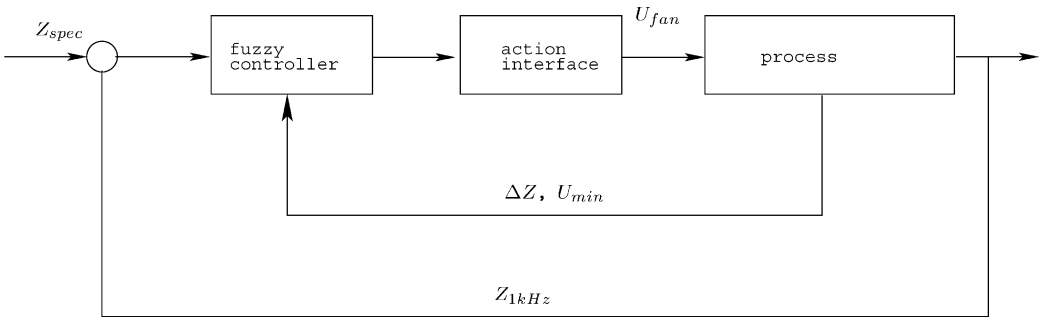

Fig. 8. Fuzzy control scheme.

range was found to be 620 ... 680 mΩ for the investigated stack. $Z_{1\,\mathrm{kHz}}$ values higher than 680 mΩ lead to avoidable ohmic losses, whereas the risk of cell flooding increases for $Z_{1\,\mathrm{kHz}}$ values lower than 620 mΩ. A linguistic variable Z_{OU} is introduced for this reason, which rates the deviation of the measured value $Z_{1\,\mathrm{kHz}}$ from the optimum range:

$$Z_{\mathrm{OU}} = \begin{cases} Z_{ll} - Z_{1\,\mathrm{kHz}} & |Z_{1\,\mathrm{kHz}} < Z_{ll} \\ 0 & |Z_{ll} \le Z_{1\,\mathrm{kHz}} \le Z_{ul}\,, \\ Z_{ul} - Z_{1\,\mathrm{kHz}} & |Z_{1\,\mathrm{kHz}} > Z_{ul} \end{cases} \tag{9}$$

where Z_{ll} and Z_{ul} are the lower and upper limits of the optimum impedance range, respectively. The linguistic variable Z_{OU} is partitioned into membership functions (see Section 3.2) as shown in Fig. 9a.

(2) The linguistic variable Z_{NA} represents the derivative of $Z_{1\,\mathrm{kHz}}$. It is approximated by the difference quotient

$$Z_{\mathrm{NA}} = \frac{Z_{1\,\mathrm{kHz}}(t_2) - Z_{1\,\mathrm{kHz}}(t_1)}{t_2 - t_1}, \tag{10}$$

where t_1 and t_2 are two consecutive time steps at which the measurement data of $Z_{1\,\mathrm{kHz}}$ are taken. Z_{NA} was introduced in order to prevent steps in the controller characteristic. If the impedance leaves its specified window, the controller reacts according to the temporal difference of the impedance. Then, the strength of the controller's reaction is proportional to this difference. Appropriate combinations of fuzzy sets of Z_{OU} and Z_{NA} are considered to prevent the controller from tending to oscillate. The membership functions of the linguistic variable Z_{NA} are shown in Fig. 9b.

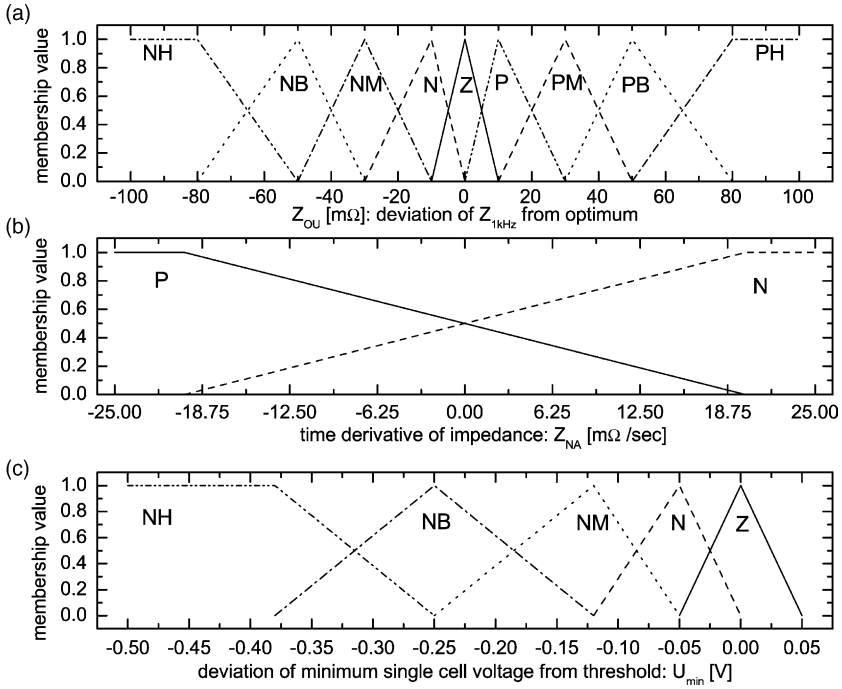

Fig. 9. Membership functions of the linguistic variables Z_{OU}, Z_{NA}, and U_{min}. The meaning of the labels corresponding to the membership functions is as follows: NH: negative huge, NB: negative big, NM: negative medium, N: negative, Z: zero, P: positive, PM: positive medium, PB: positive big, PH: positive huge.

(3) Flooding of a cell leads to an abrupt drop of the corresponding cell voltage. For example, the critical threshold value $U_{\text{threshold}}$ for the single cell voltage was found to be 0.35 V at $T = 60\,^{\circ}\text{C}$. The problem of flooding can be solved by a sharp increase of the air stoichiometry in order to extract more water. Therefore a linguistic variable $U_{\min}$ is introduced

$$U_{\min} = \min\{U_i\} - U_{\text{threshold}}; \quad \forall i \in \{1, \ldots, 15\}. \tag{11}$$

The membership functions of the linguistic variable $U_{\min}$ are shown in Fig. 9c.

A fuzzy rule base $\{R_k\}$ of TSK type (Eq. (5)) comprising 28 rules was constructed from this control scheme. The rule base is divided into three groups:

(1) Rules $R_1 \ldots R_{18}$: The antecedent includes combinations of the linguistic variables Z_{OU} and Z_{NA}. The fan voltage U_{fan} is assigned in the consequent part of the rules. For example, rule R_1 reads:

$$IF(Z_{\text{NA}}{=}N)\ \ AND(Z_{\text{OU}}{=}NH)\ \ THEN\ \ U'_{\text{fan}}{=}0.9U_{\text{fan}}.$$

(2) Rules $R_{19} - R_{23}$: The premise includes the single-cell voltages. If a single-cell voltage drops below a limiting value, the fan voltage is increased. For example, rule R_{19} reads:

$$IF(U_{\min} = NH)\ \ THEN\ \ U'_{\text{fan}} = 1.2\,U_{\text{fan}}.$$

(3) Rules $R_{24} - R_{28}$: The antecedent is active if both the fan voltage reaches its maximum value and a single-cell voltage drops below the limiting value. In this case, the controller signals that the power load has to be reduced, otherwise the fuel cell stack will be flooded with water. For example, rule R_{24} reads:

$$IF(U_{\min}{=}NH)\ \ AND(U_{\text{fan}}{=}5)\ \ THEN\ \ load'{=}0.2load.$$

7.2. Test of fuel cell stack control

The fuzzy controller was tested at a temperature of $T = 60\,^{\circ}\text{C}$ as shown in Fig. 10. $Z_{\text{ll}} = 620\,\text{m}\Omega$ and $Z_{\text{ul}} = 680\,\text{m}\Omega$ were chosen as lower and upper threshold values for the definition of Z_{spec}. The load was increased manually at times t_1, t_4 and t_6. The water production rate increased after an increase of the power load, leading to an increase of the water content of the membrane. Accordingly, the proton conductivity improves, which can be seen in the decrease of Z. The fuzzy controller reacts with an increase of fan voltage after times t_1, t_4 and t_6 because Z drops below the lower threshold value Z_{ll}. The membrane tends to become too dry at times t_2, t_3 and t_5, which is reflected by the increase of $Z_{1\,\text{kHz}}$ above the upper threshold value Z_{ul}. As a consequence, the fuzzy controller reacts with a decrease of fan voltage and the impedance decreases within several seconds.

The fuel cell stack can be controlled at $T = 60\,^{\circ}\text{C}$ up to a power level of 7.5 W (Fig. 10). A further increase of the power load leads to a drop in at least one single-cell voltage: In this case, rules $R_{24} \ldots R_{28}$ of the fuzzy rule base become active. If the fuel cell stack is operated at $T = 65\,^{\circ}\text{C}$, the impedance threshold values have to be increased. Threshold values were chosen for $Z_{\text{spec}} = [820 \ldots 940]\,\text{m}\Omega$ according to the lower water content of the membrane compared to the case with $T = 60\,^{\circ}\text{C}$. The maximum power level for which the fuel cell stack can be controlled was found to be 8 W at $T = 65\,^{\circ}\text{C}$. A decrease of the maximum power level is observed for higher temperatures.

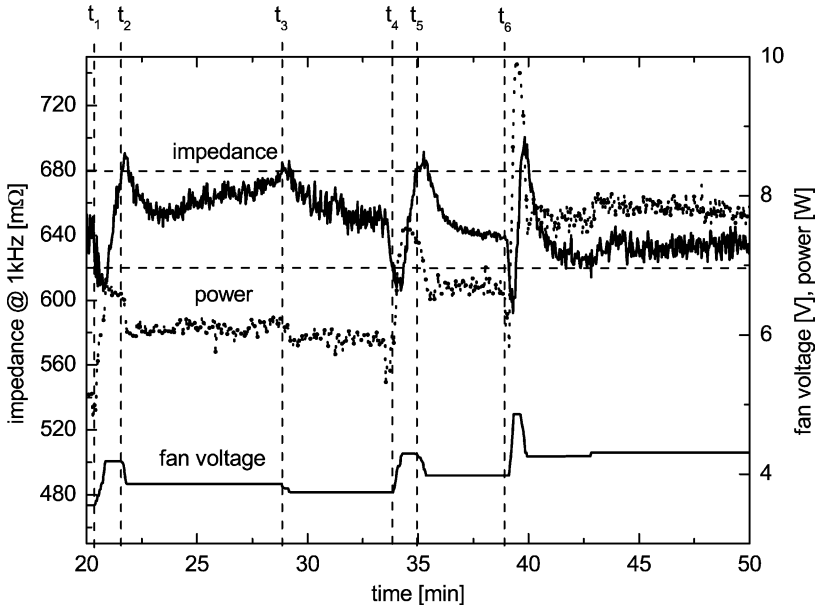

Fig. 10. Test of the control scheme at a fuel cell stack temperature of $T = 60\,^{\circ}\text{C}$.

8. Conclusion

We demonstrated the applicability of fuzzy methods for controlling miniature PEM fuel cells. The fuzzy rule base consists of empirically derived relations. This offers the advantage that water management is achieved in an efficient way. Flooding problems of the PEM fuel cell stack are prevented by monitoring the minimum single cell voltage. Drying of the PEM membrane can be avoided by monitoring the ac impedance of the fuel cell stack. A control-oriented mathematical model would have to take the dynamic two-phase problem of water transport in the PEM stack into account. The complexity of a rigorous, mathematical solution of this problem cannot be handled on-line using state-of-the-art microcontrollers. On the other hand, the fuel cell characteristics depend strongly on temperature, which is not accounted for by our present implementation of the fuzzy rule base. This temperature dependence can be introduced by simple fuzzy models with appropriate transfer characteristics. Therefore, water and thermal management can in principle be achieved by applying fuzzy logic. The cost efficiency of our control principle is yet to be demonstrated for miniature PEM fuel cells.

References

[1] J.C. Amphlett, R.M. Baumert, R.F. Mann, B.A. Peppley, P.R. Roberge, T.J. Harris, Performance modelling of the ballard mark iv solid polymer electrolyte fuel cell. Part I. mechanistic model development, J. Electrochem. Soc. 142 (1) (1995) 1–8.

[2] T.E. Springer, T.A. Zawodzinski, S. Gottesfeld, Polymer electrolyte fuel cell model, J. Electrochem. Soc. 138 (8) (1991) 2334–2342.

[3] T.F. Fuller, J. Newman, Water and thermal management in solid-polymer-electrolyte fuel cells, J. Electrochem. Soc. 140 (5) (1993) 1218–1225.

[4] D. Natarajan, T.V. Nguyen, A two-dimensional, two-phase, multicomponent, transient model for the cathode of a proton exchange membrane fuel cell using conventional gas distributors, J. Electrochem. Soc. 148 (12) (2001) A1324–A1335.

[5] Z.H. Wang, C.Y. Wang, K.S. Chen, Two-phase flow and transport in the air cathode of proton exchange membrane fuel cells, J. Power Sources 94 (2001) 40–50.

[6] M. Ceraolo, C. Miulli, A. Pozio, Modelling static and dynamic behaviour of proton exchange membrane fuel cells on the basis of electro-chemical description, J. Power Sources 113 (2003) 131–144.

[7] J. Pukrushpan, A. Stefanopoulou, H. Peng, in: Proceedings of the American Control Conference of the Modeling and control for pem fuel cell stack system, Anchorage, 2002, pp. 3117–3122.

[8] D. Boettner, G. Paganelli, Y. Guezennec, G. Rizzoni, M. Moran, Proton exchange membrane fuel cell system model for automotive vehicle simulation and control, J. Energy Res. Technol. Trans. ASME 124 (1) (2002) 20–27.

[9] H. Geyer, R. Ahluwalia, Gctool for Fuel Cell Systems Design and Analysis: User Documentation, 1998.

[10] A. Abtahi, A. Zilouchian, M. Fuchs, Design and implementation of a hierarchical control strategy for proton exchange membrane fuel cells, in: Proceedings of the Conference on Decision and Control, vol. 37, Tampa, Florida, 1998, pp. 461–462.

[11] L. Zadeh, Fuzzy sets, Information and Control (8) (1965) 338–353.

[12] D. Driankov, H.H., M. Reinfrank, An Introduction to Fuzzy Control, Springer, Berlin, 1996.

[13] B. Kosko, Neural Networks and Fuzzy Systems, Prentice Hall, Englewood Cliffs, NJ, 1992.

[14] E. Mamdani, S. Assilian, An experiment in linguistic synthesis with a fuzzy logic controller, Int. J. Man Machine Stud. 7 (1) (1975) 1–13.

[15] T. Takagi, M. Sugeno, Fuzzy identification of systems and its applications to modelling and control, IEEE Trans. Syst. Man Cybernetics 15 (1985) 116–132.

[16] T.E. Springer, T.A. Zawodzinski, S. Gottesfeld, Modeling water content effects in polymer electrolyte fuel cells, in: R.E. White, M.W. Verbrugge, J.F. Stockel (Eds.), Softbound Proceedings Series of the Modelling of batteries and fuel cells, vol. 91-10, The Electrochemical Society, Pennington, NJ, 1991, pp. 209–223.

[17] D.M. Bernardi, Water-balance calculations for solid-polymer-electrolyte fuel cells, J. Electrochem. Soc. 137 (11) (1990) 3344–3350.

[18] T.V. Nguyen, R.E. White, A water and heat management model for proton-exchange-membrane fuel cells, J. Electrochem. Soc. 140 (8) (1993) 2178–2186.

[19] T. Okada, G. Xie, M. Meeg, Simulation for water content management in membranes for polymer electrolyte fuel cells, Electrochim. Acta 43 (14–15) (1998) 2141–2155.

[20] J. Larminie, A. Dicks, Fuel Cell Systems Explained, Wiley, Baffins Lane, Chichester, 2000.

[21] G. Janssen, M. Overvelde, Water transport in the proton-exchange-membrane fuel cell: measurements of the effective drag coefficient, J. Power Sources 101 (2001) 117–125.

[22] T.E. Springer, T.A. Zawodzinkski, M.S. Wilson, S. Gottesfeld, Characterization of polymer electrolyte fuel cells using ac impedance spectroscopy, J. Electrochem. Soc. 143 (2) (1996) 587–599.